Land Cover Detection Using Temporal Features Based On Polar Representation

Thales Sehn Körting, Gilberto Câmara, Leila Maria Garcia Fonseca
Brazil's National Institute for Space Research – INPE
Image Processing Division – DPI
São José dos Campos, Brazil
Email: {thales,gilberto,leila}@dpi.inpe.br

***Abstract*—Land cover classification and change detection are important tasks in remote sensing applications. However, accurate results depend on labor-intensive analysis. Despite the great experience in image data gathering and distribution and a diversity of image processing toolboxes, it is still difficult to find techniques that provide a straightforward environment to transform multi-temporal and multi-resolution satellite image data into meaningful information. In this sense, we developed a new approach for analyzing spatio-temporal data based on a polar coordinates transformation that allows creating a new set of features which improves the classification accuracy of multi-temporal image databases. To evaluate the effectiveness of our proposed approach, we tested its ability to distinguish between different land cover classes, including cropland detection with single and double croppings over a 3-year period. The results presented an average improvement of 36.84% within the overall classification accuracy[1].**

***Keywords*-multi-temporal images; land change detection; data mining; time series; polar coordinates**

I. Introduction

We live in a dynamic environment in which changes are perceived on small, medium and large scales. Examples of environmental changes include land cover fragmentation, patch isolation, and a reduction in native species [1]. The climatic impacts are also significant, such as an increase in surface temperature and a decrease in the annual precipitation within tropical forests due to deforestation [2].

Remote sensing data represent the only reliable source of long-term observations of the Earth's surface [3], which is a good alternative for mapping land cover change. The growing amount of information provided by Earth satellites raises new possibilities in the analysis of temporal series of images. However, one problem is that remote sensing databases store millions of temporal records, which slow the detection of hidden patterns at various levels, that in certain cases are only perceived through visual inspection [4]. Thus, techniques used for data processing and information extraction are necessary.

Multi-temporal observations that use remote sensing allow to obtain relevant information about changes in the environment. This information is feasible if data related to the objects' history is available [5]. Two questions need to be addressed: "what have been the past environmental conditions?" and "when and how did such conditions change?" [6]. Change detection techniques can help to answer these questions.

Analysts interpret imagery and map changes by examining differences found in images taken at different time intervals. Rudorff et al. [7] related the increase in deforestation and converting land use from pasture and agriculture to sugarcane crops to the biofuels expansion. Southworth et al. [8] compared the trajectories of forest-cover change and the biophysical and social characteristics of the landscape using satellite images to detect land changes. Both studies evaluated past events, and the image analysis process was performed by hand. However, it is a tedious and time-consuming task to interpret long series of images using manual methods [9]. Various studies have used remote sensing techniques to analyze multi-temporal images and then to detect changes [10], [11], [12].

In agriculture applications, one challenging task is to distinguish single and double croppings among other events in satellite images [13]. Single cropping is defined as growing a crop once a year. Accordingly, double croppings are defined as growing two crops in sequence on the same field in a year; therefore a succeeding crop is planted after the preceding crop has been harvested. Because this event is recurring, its complete representation involves multi-temporal analysis. Studies that identify recurring events have used images and products from the Moderate Resolution Imaging Spectroradiometer (MODIS), which is an important source of Earth data exhibiting a high temporal resolution and a low spatial resolution [13]. This imagery records photosynthetic activity, which allows the surface analysis in time and space and provides vegetation index values (EVI2) in a spatial resolution of 250 m [14].

By following the time series with EVI2 values in a certain location, we can define a temporal profile that frequently has a cyclic behavior, as shown in Figure 1. This profile represents EVI2 values from 2000 to 2011, with a temporal resolution of 16 days. The cycles should not be considered changes, even though they contain different states of variation, such as the one from 0.1 to 0.75 between 2007 and 2008. However, techniques must be able to distinguish cycles in order to classify land cover and land change patterns. For

[1]This work relates to a Ph.D. thesis in the Remote Sensing program of INPE, presented in August 20th, 2012, named *GeoDMA: A toolbox integrating data mining with object-based and multi-temporal analysis of satellite remotely sensed imagery*.

this task, temporal profiles are used to describe transitions between objects and check the land cover change dynamics [15]. By using automatic methods, we speed up the image analysis procedures and deliver results instantly.

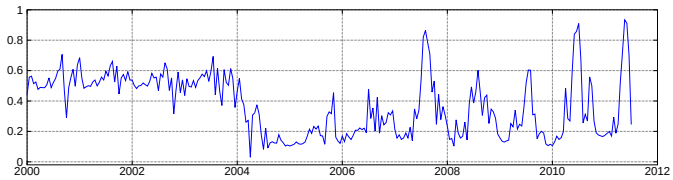

Fig. 1. EVI2 profile example from 2000 to 2011, the range of values is [0,1]. Adapted from [16].

Current feature extraction methods from profiles produce an inadequate set of properties to describe certain land patterns. The purpose of this study is to present a new approach for analyzing spatio-temporal data based on polar coordinates transformation that allows creating a new set of features which improves the classification accuracy of multi-temporal images. This set of features feeds a classification algorithm based on decision trees, which automatically creates land cover models based on a learning step. We support the proposed method for detecting land cover patterns and distinguishing single and double croppings over a 3-year time series of MODIS EVI2.

II. Methodology

The core of this work is to present the new feature set obtained from multi-temporal images. However, to obtain maps of land cover change, we based our experiments on the steps depicted in Figure 2. The main steps of the methodology include extracting features from cycles coupled with a learning phase where the domain expert trains the system with representative samples of land cover patterns. The data mining algorithm creates a classification model based on the samples, and then it is applied to the entire data set to create a land cover map.

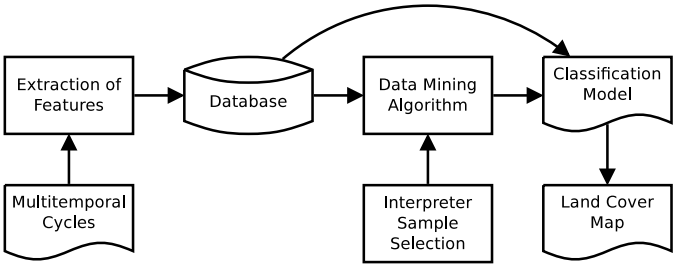

Fig. 2. Spatio-temporal analysis system for pattern detection.

At this point, we must distinguish the terms *profile* and *cycle*, although in some cases they represent the same temporal entity. Suppose we have observational data over a 5-year period with the analysis being performed yearly. In this case, one profile contains the full time series that will be divided into 5 cycles of 1 year. For example, a time series with a temporal resolution of 8 days defines a cycle with approximately 45 values per year ($\frac{365}{8} \simeq 45$). For 16 days, the number of cycles changes to 23, and so forth.

The first step of our method is to extract the cycles. In vegetation analysis the cycles are often annual, therefore this work manually defines cycles of 1 year. However, examples of automatic cycle detection include the Discrete Fourier Transform – DFT. Methods based on DFT convert the multi-temporal profile from the time domain to the frequency domain, where it is easier to identify the frequencies that compose the signal. The peaks in the power spectrum of a time series point out the cycles [17]. The work of Galford et al. [13] detects cycles by applying an annual standard deviation threshold. This threshold is selected each year from the local minimum in a bimodal histogram of standard deviation. Jonsson and Eklundh [18] use a preliminary definition of the seasonality (uni-modal or bi-modal) with timings of the growing seasons.

Given the cycles, a set of features that will appropriately characterize them is extracted and stored in a database for further access. A domain expert recognizes and selects representative samples of each land cover pattern. This sample set is used by the data mining algorithm to build a classifier model based on decision trees. We used the C4.5 algorithm [19] for classification, which is commonly used in remote sensing applications [20], [21]. Later, the cycles are classified using the model, and land cover maps are produced. Land changes are retrieved when two consecutive cycles are different.

The most important question is how to describe each cycle. Before using data to quantify or infer spatio-temporal processes, it is important to understand how the processes are represented in the data. Characterization of multi-temporal imagery provides insights into how different processes are represented by the spatial, spectral and temporal sampling of the imagery [22]. It is within this context that we developed the *Polar* representation of features to better represent cyclic patterns. These features are used with some well-known metrics, hereby called *Basic* features, which are described below.

A. Basic features

Basic features include statistical measures and phenological metrics in the case of vegetation profiles [18], [23], [24]. From each cycle, we can trace well-known statistical features such as the mean, standard deviation, minimum and maximum values and amplitude. The phenological metrics include the timing of recurring vegetation cycles (canopy emergence and senescence), the slopes of the curve, integrals and the distances between the peaks and valleys.

Figure 3 illustrates examples of Basic features.

B. Features based on Polar representation

According to Hornsby et al. [12], the standard computational models of time do not consider that certain events or phenomena may be recurring. The term cycle can also be used to capture the notion of recurring events. To support cycle's visualization, Edsall et al. [25] proposed a time-wheel legend, resembling a clock face, divided into several wedges according to the data instances.

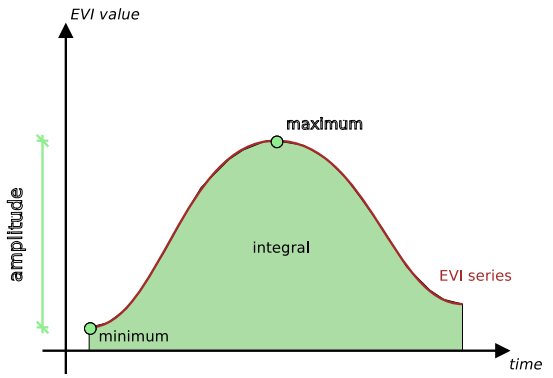

Fig. 3. Examples of *Basic* features obtained from a time series.

In our case, we adapted the time wheel legend by plotting each cycle of the profile, and by projecting values to angles in the interval [0, 2π]. Let a cycle be a function $f(x, y, T)$, where (x, y) is the spatial position of a point, T is a time interval $t_1, \ldots t_N$, and N is the number of observations in the cycle. Therefore a cycle can be visualized by a set of values $v_i \in V$, where v_i is a possible value of $f(x, y)$ in time t_i. Let its polar representation be defined by a function $g(V) \rightarrow \{A, O\}$ (A corresponds to the abscissa axis in the Cartesian coordinates, and O to the ordinate axis) where

$$a_i = v_i \cos(\frac{2\pi i}{N}) \in A, i = 1, \ldots N \tag{1}$$

and

$$o_i = v_i \sin(\frac{2\pi i}{N}) \in O, i = 1, \ldots N. \tag{2}$$

In both equations, $\frac{2\pi i}{N}$ is an arbitrary angle that depends on the acquisition date and v_i is the corresponding EVI value. If we consider $a_{N+1} = a_1$ and $o_{N+1} = o_1$, we obtain the coordinates of a closed shape. Figure 4 illustrates a cycle and its transformation to the polar coordinate system. Given such shapes, we can extract various shape and linearity metrics, such as area, perimeter, main direction, bounding ellipse, eccentricity and radius. In this scheme, a cycle with constant values outcomes a circle, and different cycles draw different shapes according to their properties. To distinguish between the existent time series features and the ones proposed in this work, all features based on the polar transformation of the cycle are named *Polar*.

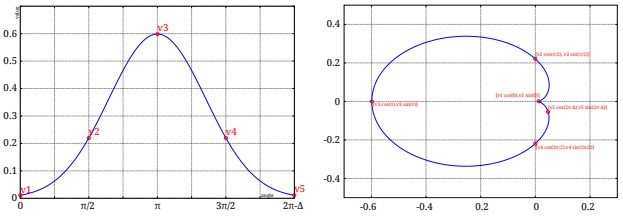

Fig. 4. When the values of the cycle are associated to a certain angle (left), the closed shape is created from its polar transformation (right).

Moreover, polar representation provides a new visualization scheme that can help us to describe the pattern represented in the cycle. It is important to state the polar transformation employed by this technique is used solely to create a closed shape, and then use this shape to obtain a new set of features. A first insight when using annual cycles suggests splitting the polar representation into 4 quadrants related to the 4 seasons. Hence, other features such as average values per season can also be computed. Another feature, called *Polar balance*, calculates the standard deviation of the area per season, which suggests the stability of the profile throughout the cycles.

From the shapes we also extract linearity features based on geometric moments [26]. The central moment μ, of order pq, from a set of points Q is defined as

$$\mu_{pq} = \sum_{x,y \in Q} (x - x_c)^p (y - y_c)^q \tag{3}$$

where (x_c, y_c) is the center of mass from Q. The feature *eccentricity* is calculated using the central moments with different orders:

$$e = \frac{\sqrt{(\mu_{20} + \mu_{02})^2 + 4\mu_{11}^2}}{\mu_{20} + \mu_{02}}. \tag{4}$$

The feature *angle of orientation* of Q is determined by

$$a = 0.5 \arctan\left(\frac{2\mu_{11}}{\mu_{20} - \mu_{02}}\right). \tag{5}$$

The feature *ellipse ratio* is obtained by $r = 1 - \frac{b}{a}$, where

$$a^+, b^- = \sqrt{\frac{2\left[\mu_{20} + \mu_{02} \pm \sqrt{(\mu_{20} - \mu_{02})^2 + 4\mu_{11}^2}\right]}{\mu_{00}}}. \tag{6}$$

All presented features for describing cyclic events (*Basic* plus *Polar*) are shown in Table I.

III. Experimental Result

The proposed set of features were employed in an experiment for detecting land cover patterns and distinguishing single and double croppings over a 3-year time series (2008 to 2010). The experiment is primarily focused on assessing the classification accuracy improvement provided with polar features. One of the objectives for identifying these cropland types is to detect extensification and intensification processes. According to Galford et al. [13], *extensification* is the increase in total row-crop agricultural area, which is measured as the annual increase from one growing season to the next. On the other hand, *intensification* describes the change from a single to double croppings pattern from one year to the next.

The data used consisted of 16-day MODIS EVI2 profiles, which is a Level 3 product (MOD13Q1), calculated from the Level 2 daily surface reflectance product (MOD09 series) [27]. The criteria for the pixel selection in these composites are based on cloud screening and data quality checks. These profiles are from the northern Mato Grosso state of Brazil (Lat. 11^{o}34'23"S, Lon. 54^{o}43'14" W). Mato Grosso contains the major frontier of row crops in Brazil, home to some of the largest contiguous row-crop plantations in the world [13].

TABLE I
TEMPORAL FEATURES FOR DESCRIBING CYCLIC EVENTS.

Name	Description	Range
Basic Features		
Amplitude	The difference between the cycle's maximum and minimum values. Small amplitude means a stable cycle.	[0, 1]
Cycle's maximum	Maximum value of the cycle. Relates the overall productivity and biomass, but it is sensitive to false highs and noise.	[0, 1]
Cycle's mean	Average value of the curve along one cycle.	[0, 1]
Cycle's minimum	Minimum value of the curve along one cycle.	[0, 1]
Cycle's std	Standard deviation of the cycle's values.	≥ 0
Cycle's sum	When using vegetation indices, the sum of values over a cycle is an indicator of the annual production of vegetation.	≥ 0
1^{st} slope maximum	Maximum value of the first slope of the cycle. It indicates when the cycle presents some abrupt change in the curve. The slope between two values relates the fastness of the greening up or the senescence phases.	[-1, 1]
Polar Features		
Angle	The main angle of the closed shape created by the polar visualization. A small angle defines a shape possibly stable along the seasons, whereas different angles point to EVI peaks in a specific season.	$[-\pi, \pi]$
Area	Area of the closed shape. A higher value indicates a cycle with high EVI values.	≥ 0
Area per Season	Partial area of the shape, proportional to some quadrant of the polar representation. High values in the summer can relate the phenological development of a cropland.	≥ 0
Circle	Returns values close to 1 when the shape is more similar to a circle. In the polar visualization, a circle means a constant feature.	[0, 1]
Eccentricity	Return values close to 0 if the shape is a circle and 1 if the shape is similar to a line.	[0,1]
Gyration radius	Equals the average distance between each point inside the shape and the shape's centroid. The more similar to a circle, the more likely the centroid will be inside it, and therefore this feature will be closer to 0.	≥ 0
Polar balance	The standard deviation of the areas per season, considering the 4 seasons. A small value can point to a constant cycle, such as the EVI of water (with a small Area), or forest (with a medium Area).	≥ 0

Each profile was divided into annual cycles because the biomass condition along an entire phenological cycle – the growing season – is approximately 1 year. Each cycle is composed of 23 values that define a growing season. The cycle starts in August of one year and finishes in July of the next year. The objects were initially identified by hand, totalizing 2035 samples over the 3-year period, with 225 and 353 samples for single and double croppings respectively, and the remaining samples (1457) to other classes, such as pasture, urban area, deforestation and forest.

The classification accuracy was analyzed using the cross-validation method, in which the samples are randomly divided into $n = 10$ folds of equal size. One fold is used for testing and the others $n - 1$ are used to train the model. The overall accuracy is obtained by averaging all the folds. Furthermore, we compared the classification accuracy between maps produced by two different feature sets: only *Basic* features and a combination of *Basic* and *Polar* features.

In a decision tree algorithm, the parameter $\min_{obj}$, which is the minimum number of objects per leave, can be used to evaluate the classification performance. According to Witten and Frank [28], this parameter has the ability to cut out tests in which almost all training samples have the same outcome. Consequently, nodes in a tree are removed unless they have at least a minimum number of cases. High $\min_{obj}$ values suggest a more generalist classification model, in which more objects are classified in the same tree path. Therefore, the experiment was also evaluated by considering the parameter $\min_{obj}$ using the Monte Carlo simulation, which performs random experiments to solve mathematical models and complex problems. This simulation's goal is to represent a real system based on the large samples theory [29]. To define a credible interval, multiple classifications were performed by varying $\min_{obj}$. For each $\min_{obj}$ value, we carried out 100 simulations by selecting random samples, which were about 30% of the total, and stored the classification accuracy for each simulation. The idea is to analyze the accuracy for both sets of features (*Basic* and *Polar* + *Basic*) in relation to $\min_{obj}$, allowing to find the most proper classification model.

We employed Monte Carlo by varying $\min_{obj}$ in the interval [1, 50] resulting in 5,000 classification models. Their accuracy values were calculated and stored. Figure 5 shows the Kappa values plotted against the parameter $\min_{obj}$. The average values were 0.57 and 0.78 for the *Basic* and *Polar* + *Basic* feature sets, respectively. It was observed that for $\min_{obj} > 30$, the accuracy for the *Basic* set of features decreased, while it remained stable at about 0.8 for the *Polar* + *Basic* features.

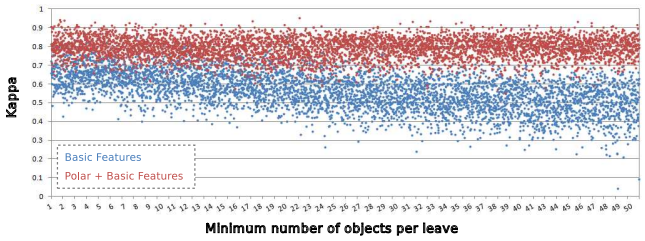

Fig. 5. Kappa values in the Monte Carlo simulation.

In Figure 6 we can observe the classification model, which employed the polar features *Gyration radius* and *Polar balance*, and the basic feature *Cycle's std*, with Kappa = 0.84. When comparing both feature sets, the improvement of adding the polar features was 36.84%.

The classification model was applied to the 3-year time series, resulting in land cover maps that describe the patterns

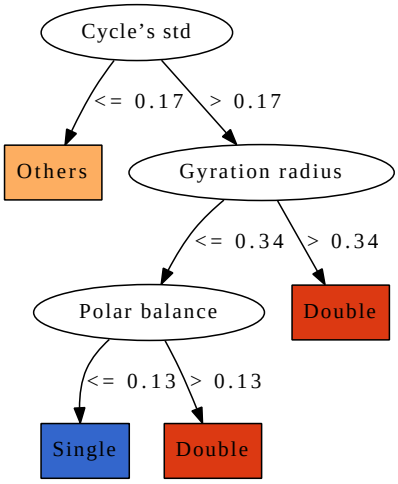

Fig. 6. Classification model using *Polar* + *Basic* features, Kappa = 0.84.

of single and double croppings from 2008 to 2010. When analyzing the trajectories of change from the cropland maps, 4 land change patterns were identified, as follows:

1) *Constant*: the land cover presented no changes along over a 3-year period;
2) *Intensification*: the land cover changed from *single* to *double* croppings;
3) *Reduction*: the land cover changed from *double* to *single* croppings;
4) *Interchange*: the land cover presented alternate behavior along the 3-year period (*double*, *single*, *double* or *single*, *double*, *single*).

The land change map obtained from the years 2008 to 2010, considered only the cropland classes, is shown in Figure 7. Figure 8 presents the individual classification for the 3 years.

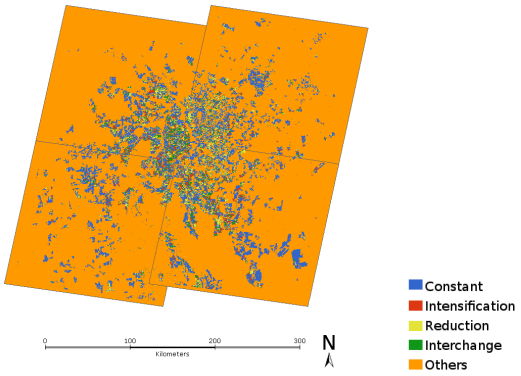

Fig. 7. Land change map produced from land cover maps for the years 2008, 2009 and 2010.

IV. Conclusion

Land use and cover maps derived from remotely sensed data are a valuable source of information about the status and trends of natural and anthropogenic impacts on the Earth [30]. According to Udelhoven [4], time series analysis distinguishes gradual and abrupt changes and inter-annual variations of phenology caused externally, through changes in climate, land cover or land degradation.

In this work, we proposed a method to detect land cover patterns using EVI2 MODIS time series and a set of features based on statistical metrics and polar representation. Such representation for cycles created closed shapes relating the temporal behavior of a cycle to angles in the interval $[0, 2\pi]$, making it possible to extract features that accurately represent land cover patterns. Thus, we employed an automatic method based on image analysis and data mining techniques to detect land cover patterns within satellite time series. To illustrate the potential of our methodology, we presented an experiment to distinguish between single and double croppings. Evaluation tests using the Monte Carlo simulation and Kappa indices stated that the classification performance was improved by 36.84% for distinguishing single and double croppings from other land cover types.

This work was developed using the C++ library TerraLib [31]. For future studies, we intend to explore these features to identify land changes by analyzing consecutive cycles where the changes are observed.

Acknowledgment

We acknowledge CNPq and CAPES (Brazil), who partially funded this research.

References

[1] J. Metzger, A. Martensen, M. Dixo, L. Bernacci, M. Ribeiro, A. Teixeira, and R. Pardini, "Time-lag in biological responses to landscape changes in a highly dynamic Atlantic forest region," *Biological Conservation*, vol. 142, no. 6, pp. 1166–1177, 2009. [Online]. Available: http://linkinghub.elsevier.com/retrieve/pii/S0006320709000780

[2] C. Nobre, P. Sellers, and J. Shukla, "Amazonian deforestation and regional climate change," *Journal of Climate*, vol. 4, 1991.

[3] B. Bradley, R. Jacob, J. Hermance, and J. Mustard, "A curve fitting procedure to derive inter-annual phenologies from time series of noisy satellite NDVI data," *Remote Sensing of Environment*, vol. 106, no. 2, pp. 137–145, Jan. 2007. [Online]. Available: http://linkinghub.elsevier.com/retrieve/pii/S0034425706003014

[4] T. Udelhoven, "TimeStats: A software tool for the retrieval of temporal patterns from global satellite archives," *Earth*, vol. 4, no. 2, pp. 310–317, 2011.

[5] J. Mota, M. Escada, O. Bittencourt, L. Fonseca, and L. Vinhas, "Case-based reasoning for eliciting the evolution of geospatial objects," in *Conference on Spatial Information Theory*. Berlin, Heidelberg: Springer-Verlag, 2009, p. 88.

[6] J. Rasinmaki, "Modelling spatio-temporal environmental data," *Environmental Modelling & Software*, vol. 18, pp. 877–886, 2003.

[7] B. Rudorff, M. Adami, D. Aguiar, A. Gusso, W. Silva, and R. Freitas, "Temporal series of EVI/MODIS to identify land converted do sugarcane," in *IGARSS*. Cape Town, South Africa: IEEE, 2009.

[8] J. Southworth, H. Nagendra, and C. Tucker, "Fragmentation of a Landscape: incorporating landscape metrics into satellite analyses of land-cover change," *Landscape*, vol. 27, no. 3, pp. 253–269, 2002.

[9] W. Boulila, I. Farah, K. Ettabaa, B. Solaiman, and H. Ghézala, "A data mining based approach to predict spatiotemporal changes in satellite images," *International Journal of Applied Earth Observation and Geoinformation*, vol. 13, no. 3, pp. 386–395, Jun. 2011. [Online]. Available: http://linkinghub.elsevier.com/retrieve/pii/S0303243411000250

[10] S. Boriah, V. Kumar, M. Steinbach, C. Potter, and S. Klooster, "Land cover change detection: A case study," in *International conference on knowledge discovery and data mining*, 2008, pp. 857–865.

[11] C. Potter, V. Genovese, P. Gross, S. Boriah, M. Steinbach, and V. Kumar, "Revealing land cover change in california with satellite data," *EOS*, vol. 88, no. 26, 2007.

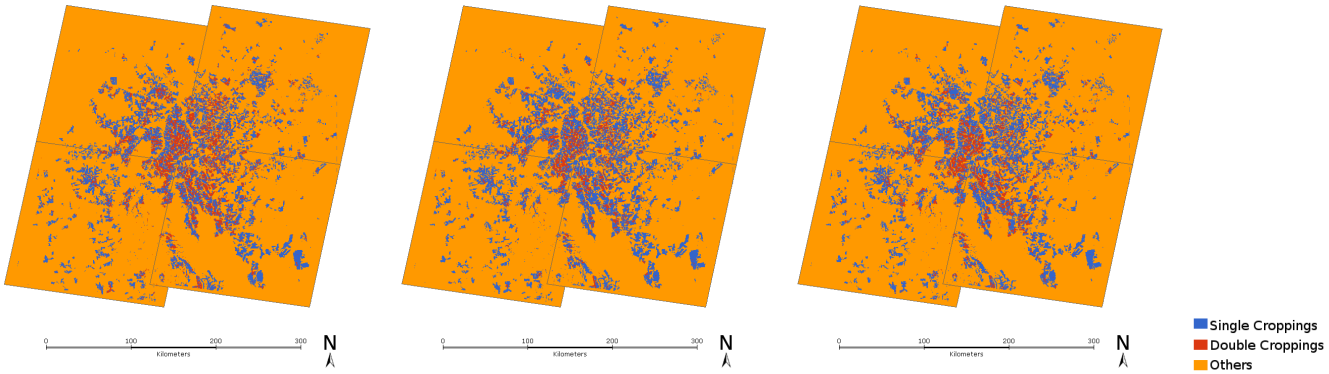

Fig. 8. Classification of single and double croppings for the years 2008, 2009, and 2010 (left to right), in the Mato Grosso state.

[12] K. Hornsby, M. Egenhofer, and P. Hayes, "Modeling Cyclic Change," *Advances in Conceptual Modeling*, vol. 1727, no. 1, pp. 98–109, 1999.

[13] G. Galford, J. Mustard, J. Melillo, A. Gendrin, C. Cerri, and C. Cerri, "Wavelet analysis of MODIS time series to detect expansion and intensification of row-crop agriculture in Brazil," *Remote Sensing of Environment*, vol. 112, no. 2, pp. 576–587, Feb. 2008. [Online]. Available: http://linkinghub.elsevier.com/retrieve/pii/S0034425707002258

[14] A. Huete, K. Didan, T. Miura, E. Rodriguez, X. Gao, and L. Ferreira, "Overview of the radiometric and biophysical performance of the MODIS vegetation indices," *Remote Sensing of Environment*, vol. 83, no. 1-2, pp. 195–213, Nov. 2002. [Online]. Available: http://linkinghub.elsevier.com/retrieve/pii/S0034425702000962

[15] R. Freitas and Y. Shimabukuro, "Combining wavelets and linear spectral mixture model for MODIS satellite sensor time-series analysis," *Journal of Computational Interdisciplinary Sciences*, vol. 1, no. 1, pp. 51–56, 2008.

[16] R. Freitas, E. Arai, M. Adami, A. Souza, F. Sato, Y. Shimabukuro, R. Rosa, L. Anderson, and B. Rudorff, "Virtual laboratory of remote sensing series: visualization of MODIS EVI2 data set over South America," *Journal of Computational Interdisciplinary Sciences*, vol. 2, pp. 57–64, 2011.

[17] P. Tan, M. Steinbach, V. Kumar, C. Potter, S. Klooster, and A. Torregrosa, "Finding Spatio-Temporal Patterns in Earth Science Data," *Earth Science*, pp. 1–12, 2001.

[18] P. Jonsson and L. Eklundh, "TIMESAT: A program for analyzing time-series of satellite sensor data," *Computers & Geosciences*, vol. 30, no. 8, pp. 833–845, Oct. 2004. [Online]. Available: http://linkinghub.elsevier.com/retrieve/pii/S0098300404000974

[19] J. Quinlan, *C4.5: programs for machine learning*. San Mateo, CA: Morgan Kaufmann, 1993. [Online]. Available: http://books.google.com/books?id=HExncpjbYroC

[20] M. Silva, G. Câmara, M. Escada, and R. Souza, "Remote-sensing image mining: detecting agents of land-use change in tropical forest areas," *International Journal of Remote Sensing*, vol. 29, pp. 4803–4822, 2008.

[21] M. Vieira, A. Formaggio, C. Rennó, C. Atzberger, D. Aguiar, and M. Mello, "OBIA and Data Mining applied to a remotely sensed Landsat time-series to map sugarcane over large areas," *Remote Sensing of Environment*, vol. 123, pp. 553–562, Aug. 2012. [Online]. Available: http://linkinghub.elsevier.com/retrieve/pii/S0034425712001800

[22] C. Small, "Spatiotemporal dimensionality and time-space characterization of vegetation phenology from multitemporal MODIS EVI," in *MultiTemp*. IEEE, 2011, pp. 65–68. [Online]. Available: http://ieeexplore.ieee.org/xpls/abs_all.jsp?arnumber=6005049

[23] C. Atzberger and P. Eilersb, "Evaluating the effectiveness of smoothing algorithms in the absence of ground reference measurements," *International Journal of Remote Sensing*, vol. 32, no. 13, 2011.

[24] C. Hüttich, U. Gessner, M. Herold, B. Strohbach, M. Schmidt, M. Keil, and S. Dech, "On the suitability of MODIS time series metrics to map vegetation types in dry savanna ecosystems," *Remote Sensing*, vol. 1, no. 4, pp. 620–643, Sep. 2009. [Online]. Available: http://www.mdpi.com/2072-4292/1/4/620/

[25] R. Edsall, M. Kraak, A. MacEachren, and D. Peuquet, "Assessing the effectiveness of temporal legends in environmental visualization," *Proceedings of GIS/LIS*, pp. 677–85, 1997.

[26] M. Stojmenovic, A. Nayak, and J. Zunic, "Measuring linearity of planar point sets," *Pattern Recognition*, vol. 41, no. 8, pp. 2503–2511, Aug. 2008. [Online]. Available: http://linkinghub.elsevier.com/retrieve/pii/S0031320308000381

[27] E. Vermote, N. Saleous, and C. Justice, "Atmospheric correction of MODIS data in the visible to middle infrared: first results," *Remote Sensing of Environment*, vol. 83, pp. 97–111, 2002.

[28] I. Witten and E. Frank, *Data Mining: Practical machine learning tools and techniques*, 2nd ed. San Francisco, CA: Diane Cerra, 2005.

[29] R. Rubinstein and D. Kroese, *Simulation and the Monte Carlo method*. New Jersey: Wiley-interscience, 2008.

[30] J. Knight and M. Voth, "Mapping Impervious Cover Using Multi-Temporal MODIS NDVI Data," *Selected Topics in Applied Earth Observations and Remote Sensing*, vol. 4, no. 99, pp. 1–7, 2011. [Online]. Available: http://ieeexplore.ieee.org/xpls/abs_all.jsp?arnumber=5508338

[31] G. Câmara, L. Vinhas, K. Ferreira, G. Queiroz, R. Souza, A. Monteiro, M. Carvalho, M. Casanova, and U. Freitas, "TerraLib: An open source GIS library for large-scale environmental and socio-economic applications," *Open Source Approaches in Spatial Data Handling*, vol. 2, pp. 247–270, 2008. [Online]. Available: http://www.springerlink.com/index/K505665570287237.pdf